



Title	Three-variable reversible Gray–Scott model
Author(s)	Mahara, Hitoshi; Suematsu, Nobuhiko J.; Yamaguchi, Tomohiko; Ohgane, Kunishige; Nishiura, Yasumasa; Shimomura, Masatsugu
Citation	The Journal of Chemical Physics, 121(18), 8968-8972 https://doi.org/10.1063/1.1803531
Issue Date	2004
Doc URL	http://hdl.handle.net/2115/5428
Rights	Copyright © 2004 American Institute of Physics
Type	article
File Information	JCP121-18.pdf



[Instructions for use](#)

Three-variable reversible Gray–Scott model

Hitoshi Mahara

National Institute of Advanced Industrial Science and Technology (AIST), Higashi 1-1-1, Tsukuba 305-8565, Japan and CREST, Japan Science and Technology Agency (JST), Motomachi 4-1-8, Kawaguchi, Saitama 332-0012, Japan

Nobuhiko J. Suematsu and Tomohiko Yamaguchi^{a)}

National Institute of Advanced Industrial Science and Technology (AIST), Higashi 1-1-1, Tsukuba 305-8565, Japan and Graduate School of Pure and Applied Sciences, University of Tsukuba, Tsukuba 305-8571, Japan

Kunishige Ohgane

National Institute of Advanced Industrial Science and Technology (AIST), Higashi 1-1-1, Tsukuba 305-8565, Japan

Yasumasa Nishiura

Research Institute for Electronic Science, Hokkaido University, Kita-ku, Sapporo 060-0812, Japan

Masatsugu Shimomura

Nanotechnology Research Center, Research Institute for Electronic Science, Hokkaido University, Kita-ku, Sapporo 010-0021, Japan

(Received 28 June 2004; accepted 11 August 2004)

Even though the field of nonequilibrium thermodynamics has been popular and its importance has been suggested by Demirel and Sandler [J. Phys. Chem. B **108**, 31 (2004)], there are only a few investigations of reaction-diffusion systems from the aspect of thermodynamics. A possible reason is that model equations are complicated and difficult to analyze because the corresponding chemical reactions need to be reversible for thermodynamical calculations. Here, we introduce a simple model for calculation of entropy production rate: a three-variable reversible Gray–Scott model. The rate of entropy production in self-replicating pattern formation is calculated, and the results are compared with those reported based on the Brusselator model in the context of biological cell division. © 2004 American Institute of Physics. [DOI: 10.1063/1.1803531]

Many pattern formations in nonequilibrium systems, especially in reaction-diffusion systems have been investigated.^{1–3} In these models for reaction-diffusion systems, backward chemical reactions are ordinarily neglected because a nonequilibrium system is set so far away from equilibrium that the rates of the forward chemical reactions are much larger than those of the backward reactions. Thanks to this assumption, nonlinear chemical reaction models become relatively simple,^{4–7} and mathematical analyses and simulation of pattern formations become easy to be investigated.^{8–11} However, this assumption prevents us from calculating the entropy production rates in the course of pattern formation. Even though the existence of dissipative structures was discussed theoretically by Nicolis and Prigogine¹² from the viewpoint of thermodynamics, and its importance was suggested,¹³ this assumption prevents one from investigating the thermodynamics of pattern formation.

However, in the early era in the history of nonequilibrium studies, there appeared some thermodynamical investigations for chemical oscillations or pattern formations.^{14–17} In a reaction system that consists of the reversible Oregonator model, Irvin and Ross¹⁴ reported that the entropy produc-

tion rate averaged over one cycle of oscillations is not always higher than that of the stable steady state. In a reaction-diffusion system, which consists of the reversible Brusselator model, Hanson¹⁵ reported a discontinuous increase in the entropy production rate in accordance with the discontinuous transition of one-dimensional (1D) pattern configuration by increasing the system size; he pointed out an entropic advantage of biological cell division.

Recently, we proposed a concept of “self-organization of hierarchy” after self-organization in biological systems.¹⁸ This concept deals with a self-organizing process of hierarchy in a system and emphasizes the importance of the mutual assistance between self-assembly near equilibrium conditions and dissipative-structure formation under the conditions far from equilibrium. The dynamic interactions should also be considered between the system and its environment.¹⁹ In this framework, it is important to evaluate how far from equilibrium the self-organization occurs. That is, we need a quantitative measure that indicates the distance of the system from the equilibrium state, such as the entropy production rate in the steady state. But unfortunately, all reversible models proposed so far do not suit this purpose, because the constants in the environment of an open system cannot be constant anymore for describing the dynamics of hierarchic systems, and consequently, the number of variables to be handled must increase. Therefore, we introduce

^{a)}Author to whom correspondence should be addressed. Electronic mail: tomo.yamaguchi@aist.go.jp

here a simple model that does not need to increase the number of variables for hierarchic description and is convenient for thermodynamic consideration.

A model we propose here is a reversible Gray–Scott model. The reversible Gray–Scott model is an expansion of the Gray–Scott model and is derived from a set of the following two reversible chemical reactions:



The original Gray–Scott model corresponds to the two irreversible reactions, where the product P is an inert product. So the original model has two variables, U and V . However, we suppose that the product is not inert and the reactions are reversible. Then the system has three variables: U , V , and P . As in the original model, U is fed to the system and all species are removed from the system by the flow. Only the feeding terms depend on the external fields. Thus the model equation becomes

$$\begin{aligned} \frac{dU}{dt} &= -k_1 UV^2 + f(1-U) + k_{-1} V^3, \\ \frac{dV}{dt} &= k_1 UV^2 - (f+k_2)V - k_{-1} V^3 + k_{-2} P, \\ \frac{dP}{dt} &= k_2 V - k_{-2} P - fP, \end{aligned} \quad (2)$$

where f is the feeding rate constant, k_1 and k_2 are the reaction rate constants of the first and the second forward reactions, respectively, and k_{-1} and k_{-2} are the rate constants of the first and the second backward reactions, respectively. For simplicity, we choose the constant k_1 unity after the original model: $k_1 = 1$. Also, both the first and the second backward reaction rates are equal and considered as the constant parameter: $k_{-1} = k_{-2} \equiv k$. Thus the system is governed by the three parameters: k_2 , f , and k_r .

The system has a stable steady state $(U, V, P) = (1.0, 0.0, 0.0)$ for all positive parameters. This steady state means that the system reaches the equilibrium state and the concentrations of chemical species do not change by the feeding. Since there appear neither patterns nor concentration changes of components that change the entropy of the system, we call this spatially homogeneous solution the equilibrium solution.

The dependence of the model on the three parameters k_2 , f , and k_r is shown in the phase diagrams in Fig. 1. In this phase diagram on the f - k_2 plane [Fig. 1(a)], the solid line represents a saddle-node bifurcation line and the dashed one represents a Hopf bifurcation line. The saddle-node bifurcation line is given as a function of the feeding rate f and the backward reaction rate k_r :

$$\begin{aligned} k_2 = F(f, k_r) &= (f + k_r) \left[-1 + \frac{k_r}{2} + \sqrt{\left(\frac{k_r}{2}\right)^2 + \frac{1}{4f}} \right], \\ f > 0, \quad k_2 > 0. \end{aligned} \quad (3)$$

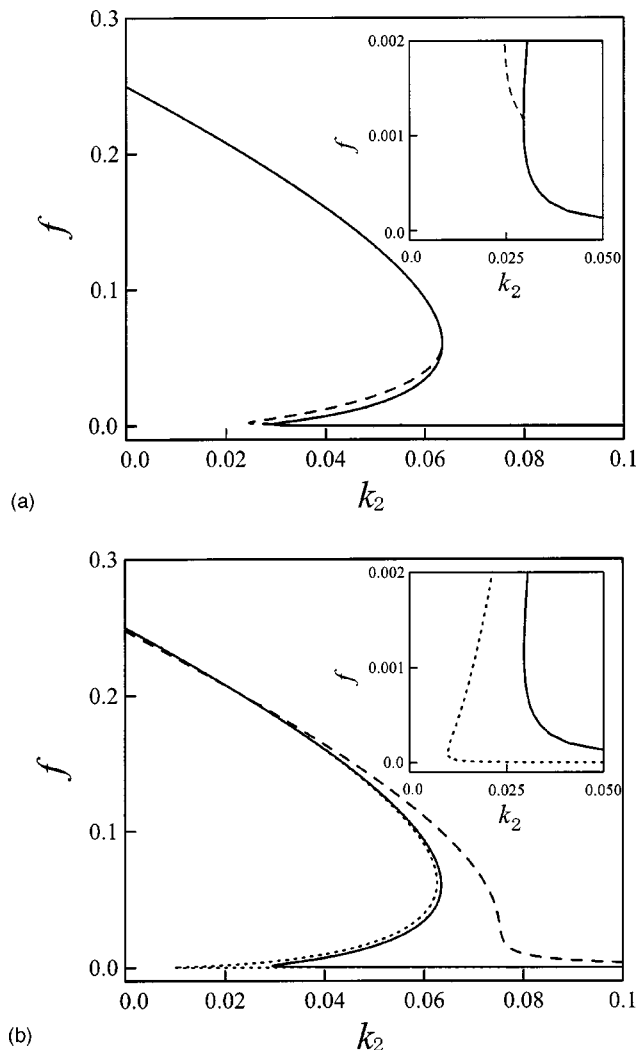


FIG. 1. (a) A phase diagram when the backward reaction rate $k_r = 1.0 \times 10^{-3}$. The solid line is the saddle-node bifurcation line. The dashed line is the Hopf bifurcation line. The inset shows the expansion near the extremal point corresponding to the lower f . The Hopf bifurcation line is connected to the saddle-point at the extremal points. (b) Saddle-node bifurcation lines. Dotted line: $k_r = 1.0 \times 10^{-4}$, solid line: $k_r = 1.0 \times 10^{-3}$, and dashed line: $k_r = 1.0 \times 10^{-2}$. When $k_r = 1.0 \times 10^{-2}$, there is no Hopf bifurcation line. All saddle-node bifurcation lines go asymptotic to $f=0$ as k_2 goes to the infinity.

This line, given as a function of f , has two extremal points where it joins the Hopf line. On the left side of the saddle-node bifurcation line [$k_2 < F(f, k_r)$], the system has three steady points: the equilibrium solution, a saddle point, and a nonequilibrium steady point. The nonequilibrium steady point is stable, and the system has two stable steady points. However, in the region enclosed by the solid and the dotted lines, the nonequilibrium steady point becomes unstable. To the right of the solid line [$k_2 > F(f, k_r)$], the system has only the equilibrium solution. This diagram goes asymptotically to that of the original Gray–Scott model when the backward reaction rate k_r goes to 0.0. On the other hand, the diagram becomes different from the original one with an increase of the backward reaction rate; the values f and k_2 of the lower extremal point increase with an increase of the backward reaction rate and simultaneously the two extremal points be-

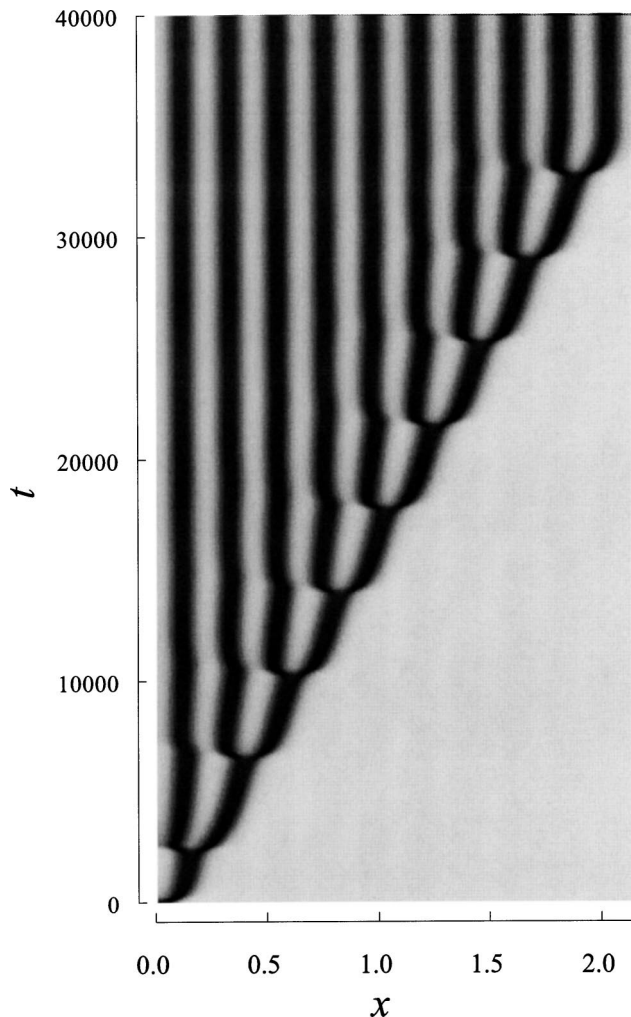


FIG. 2. A space-time plot of the one-dimensional system. The Gray level shows the concentration of U from 0.0 (black) to 1.0 (white). The constant parameters: $k_r=1.0\times 10^{-3}$, $k_2=0.06$, and $f=0.03$. The time resolution $dt=0.1$, the space resolution $dx=0.005$, and the diffusion coefficients: $D_U=2.0\times 10^{-5}$, $D_V=1.0\times 10^{-5}$, and $D_P=1.0\times 10^{-6}$.

come closer. Finally, these extrema disappear when $k_r=0.009346$. This annihilation makes the Hopf line disappear, and only the saddle-node bifurcation line remains.

Numerically, the model equations are solved in a 1D reaction-diffusion system by the 3rd-Runge-Kutta method and the finite difference method for the linear diffusion terms. The system consists of 431 sites and has the Neumann boundary conditions. The system size N is $430dx=2.15$, where $dx=0.005$ is the grid length.

Initially, all sites of the system are set to the equilibrium solution $(U, V, P) = (1.0, 0.0, 0.0)$. In order to produce a pattern, we perturb 20 sites from the left boundary by setting their initial values as $(U, V, P) = (0.5, 0.25, 0.0)$. The space-time plot of the 1D system is shown in Fig. 2. At the beginning, one pulse is generated by the initial perturbations. After a while, this pulse duplicates. The pulse at the left boundary becomes stable and does not self-replicate anymore. The other pulse self-replicates again. In this way, the number of pulses increases one by one, and the domain is covered by the pulses expanding toward the right vacant space. The pulse remaining behind the front becomes stable immedi-

ately after self-replication with the same wavelength ($L=0.215$) as that of the stable pulse. We call this wavelength a cozy wavelength and the pulse a cozy pulse. After the system is filled by the cozy pulses, the pattern becomes stable. Only a front pulse can self-replicate because of sufficient supply of substrates from the vacant surroundings; a general setting for this self-replicating dynamics is given mathematically.²⁰

The entropy production rate of the whole process of the present 1D system is calculated as follows. The entropy production rate of this reaction-diffusion system (σ) is given by the sum of space integration of two components:

$$\sigma = \sigma_{\text{chem}} + \sigma_{\text{diff}}. \quad (4)$$

The first component on the right side of Eq. (4) is the space integration of the entropy production rate per unit volume due to chemical reactions

$$\sigma_{\text{chem}} = \int \sum_j (v_j^+ - v_j^-) \ln(v_j^+/v_j^-) dx, \quad (5)$$

where v_j^+ and v_j^- are the reaction rates in the forward and the backward directions of the j th chemical reaction. When a chemical reaction locally reaches equilibrium, the entropy production rate of the chemical reaction at the local point

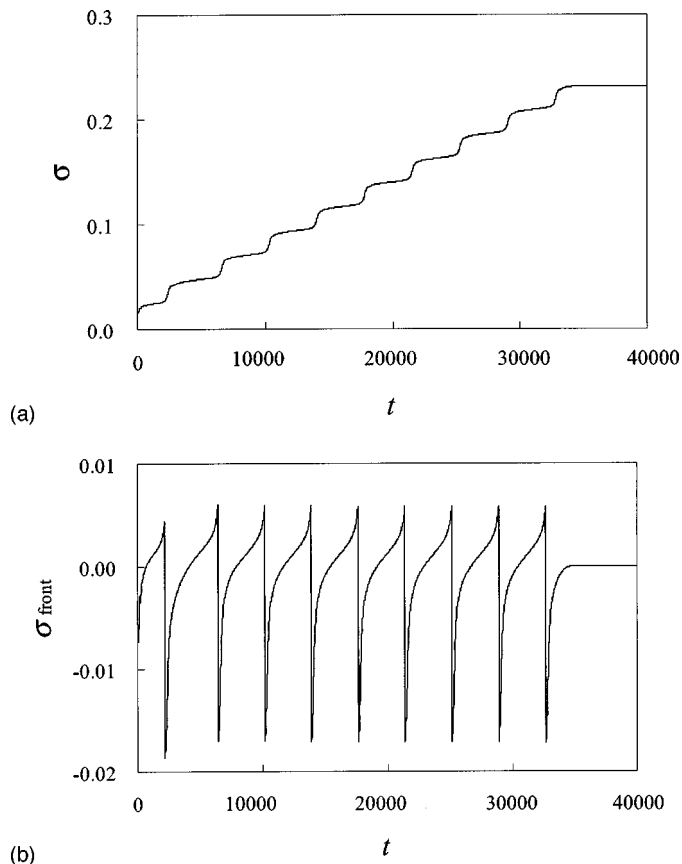


FIG. 3. (a) The entropy production rate corresponding to Fig. 2. (b) The entropy production rate of self-replicating front, σ_{front} : for its definition, see Eq. (7) and text.

should be 0.0. The second component on the right side of Eq. (4) is the spatial integral of the entropy production rate per unit volume due to diffusion:

$$\begin{aligned}\sigma_{\text{diff}} &= \int \sum_l D_l \left(\frac{\partial \ln(\Gamma_l)}{\partial x} \right) \left(\frac{\partial \Gamma_l}{\partial x} \right) dx \\ &= \int \sum_l \frac{D_l}{\Gamma_l} \left(\frac{\partial \Gamma_l}{\partial x} \right)^2 dx,\end{aligned}\quad (6)$$

where Γ_l is the concentration of the l th chemical species. In this report, we set the gas constant R unity for simplicity.

The time series of the entropy production rate of the 1D system is plotted in Fig. 3(a). Before the initial perturbations are given to the system, the system is in an equilibrium state, and the entropy production rate of the system is 0.0. At the beginning of the simulation, the entropy production rate has some finite value because of the perturbations. Then the entropy production rate increases stepwise with time. The rapid increase of this rate corresponds to the self-replication of the pulse. Finally, the rate reaches a constant value when the pattern reaches the steady state.

In order to discuss clearly the entropy production rate of a self-replicating pulse, we introduce the following value that is a measure of the entropy production rate of the self-replicating front of the system:

$$\sigma_{\text{front}} = \sigma - m\sigma_{\text{cp}}, \quad (7)$$

where m is the number of pulses in space that is counted by the number of minima in U , and σ_{cp} is the entropy production rate of a cozy pulse. The entropy production rate of a cozy pulse is defined by the values related to the final steady state:

$$\begin{aligned}\sigma_{\text{cp}} &= (\text{the final entropy production rate of the whole} \\ &\quad \text{system}) / (\text{the final number of pulses}) \\ &= 0.231/10 = 0.0231.\end{aligned}\quad (8)$$

Thus, σ_{front} has such a physical meaning that shows the entropy production rate of the self-replicating front relative to the rate of a cozy pulse.

The value of σ_{front} changes periodically in accordance with the self-replicating process. During the process for the front pulse to propagate toward the right, its entropy production rate increases monotonously. The positive value of σ_{front} means that the entropy production rate of the front pulse becomes larger than that of the cozy pulse. When the front pulse duplicates, which is known by the splitting of the minima in the pulse, there appears a discontinuity in the value of σ_{front} . At this moment, σ_{front} turns to negative, i.e., the entropy production rate of each replicated pulse is smaller than that of the cozy pulse. These two pulses grow gradually, and when the value of σ_{front} becomes zero, these pulses have almost the same entropy production rate as that of the cozy pulse. As seen in Fig. 2, one of the two pulses (the left one) becomes a stable cozy pulse immediately. Then the contribution of this pulse to the value of σ_{front} becomes

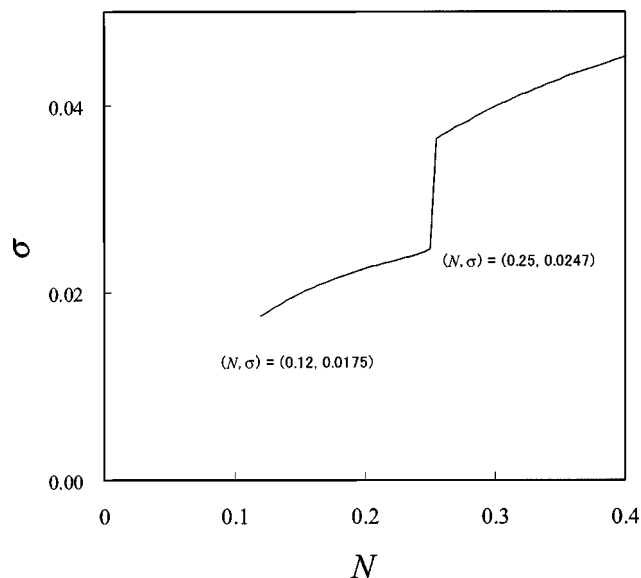


FIG. 4. The entropy production rate against the system size. When the system size $N < 0.12$, no pulse exists. When the system size $0.12 \leq N \leq 0.25$, a single stable pulse exists. When the system size $N > 0.25$, two stable pulses exist in the system.

zero. On the other hand, the right pulse goes into the self-replicating process again. This scenario is repeated until the system is filled with the pulse pattern.

Now, we discuss the difference between Hanson's work¹⁵ and the present work as an example. He calculated the entropy production rate of a reversible Brusselator distributed in a 1D space by increasing the system size and found that the entropy production rate changes discontinuously at a certain point where there appears a discontinuous change in the wavy profile of the system. This observation led him to point out a similarity concerning self-replication between his system and a living cell and to suggest the following entropy hypothesis: just before this point of discontinuity, the entropy production rate of the system (one cell) might become greater than the sum of two halves—if so, “at this point it would be energetically favorable for the cell to divide because the resulting two-cell composite would dissipate less energy.”¹⁵ We checked this hypothesis in the present system by changing the system size (Fig. 4), similar as in his work but using Neumann boundary conditions. A single pulse can be stable when the system size N is $0.12 \leq N \leq 0.25$. The entropy production rate is an increasing function of N and is 0.0175 and 0.0247 when $N = 0.12$ and 0.25, respectively. So the entropy production rate of the largest pulse is smaller than the twice of its half or of the minimum pulse. Therefore, the entropy production rate of one pulse cannot grow to twice that of any stable pulse. Actually, as already shown in Fig. 3(b), a front pulse in the 1D system grows till the entropy production rate of the front pulse σ_{front} reaches 0.00595, i.e., its entropy production rate is 0.02905 ($=0.00595 + 0.0231$). This is the maximum entropy production rate of a single pulse, and is considerably smaller than twice the minimum of the stable pulse of $0.035 (=0.0175 \times 2)$. Therefore, at the moment the pulse duplicates, the entropy production rate of the self-replicating pulse [Fig. 3(b)]

has the same feature that the pulse duplicates as increasing the system size (Fig. 4). So we conclude that the entropy production rate of one pulse cannot grow to be twice that of any stable pulse in the present self-replicating process. The hypothesis of the entropy-driven self-replication is not general but system-dependent; at least in the present system, the entropy hypothesis is not satisfied.

In summary, we propose a different simple model: the reversible Gray–Scott model to calculate the entropy production rate of pattern formation processes. Its phase diagrams are obtained, and the model is applied to the self-replicating pulses. The pulse-replicating process at the peripheral region is traced well by the entropy production rate. We believe that the present model has two advantages. The first advantage is the same as of the original Gray–Scott model; though so simple, the system shows a number of patterns (lines, dots, and chaotic patterns, etc., in 2D simulations²¹) depending on the three parameters: k_2 , f , and k_r . It is therefore a good model to compare and to discuss various pattern formation processes from the aspect of thermodynamics. The second advantage is that when constructing a nested system, the present model needs to change the feed terms only in order to take into account the interaction among nested sub-systems. With these advantages, the three-variable Gray–Scott model is expected to be a powerful tool for investigating the thermodynamics of pattern dynamics and of self-organization of hierarchy in an open system.

ACKNOWLEDGMENT

H.M. and T.Y. thank Dr. J. A. Pojman and Dr. M. Menzinger for reading the manuscript.

- ¹H. Guo, L. Li, H. Wang, and Q. Ouyang, *Phys. Rev. E* **69**, 056203 (2004).
- ²K. J. Lee, W. D. McCormick, Q. Ouyang, and H. L. Swinney, *Science* **261**, 192 (1993).
- ³P. De Kepper, V. Castets, E. Dulos, and J. Boissonade, *Physica D* **49**, 161 (1991).
- ⁴I. Prigogine and R. Lefever, *J. Chem. Phys.* **48**, 1695 (1968).
- ⁵R. J. Field and R. M. Noyes, *J. Am. Chem. Soc.* **96**, 2001 (1974).
- ⁶J. P. Keener and J. J. Tyson, *Physica D* **21**, 307 (1986).
- ⁷P. Gray and S. K. Scott, *Chem. Eng. Sci.* **39**, 1087 (1984).
- ⁸I. R. Epstein and J. A. Pojman, *An Introduction to Nonlinear Chemical Dynamics—Oscillations, Waves, Patterns and Chaos* (Oxford University Press, New York, 1998).
- ⁹J. E. Pearson, *Science* **261**, 189 (1993).
- ¹⁰H. Mahara, T. Yamaguchi, and Y. Amagishi, *Chem. Phys. Lett.* **317**, 23 (2000).
- ¹¹Y. Nishiura and D. Ueyama, *Physica D* **150**, 137 (2001).
- ¹²G. Nicolis and I. Prigogine, *Self-Organization in Non-Equilibrium System* (Wiley, New York, 1977).
- ¹³Y. Demirel and S. I. Sandler, *J. Phys. Chem. B* **108**, 31 (2004).
- ¹⁴B. R. Irvin and J. Ross, *J. Chem. Phys.* **89**, 1064 (1988).
- ¹⁵M. P. Hanson, *J. Chem. Phys.* **60**, 3210 (1974).
- ¹⁶K. Lindgren and B. A. G. Mansson, *Z. Naturforsch.* **41a**, 1111 (1986).
- ¹⁷B. A. G. Mansson, *Z. Naturforsch.* **40a**, 877 (1985).
- ¹⁸T. Yamaguchi, N. J. Suematsu, and H. Mahara, *ACS Symp. Ser.* **869**, 16 (2004).
- ¹⁹A. S. Mikhailov and V. Calenbuhr, *From Cells to Societies: Models of Complex Coherent Action* (Springer, Berlin, 2002).
- ²⁰S. Ei, Y. Nishiura, and K. Ueda, *Jpn. J. Ind. Appl. Math.* **18**, 181 (2001).
- ²¹H. Mahara *et al.* (unpublished).